Small Bright Charged Colloidal Quantum Dots

Wei Qin, Heng Liu, and Philippe Guyot-Sionnest*

James Franck Institute, The University of Chicago, 929 East 57th Street, Chicago, Illinois 60637, United States

ABSTRACT Using electrochemical charge injection, the fluorescence lifetimes of negatively charged core/shell CdTe/CdSe QDs are measured as a function of core size and shell thickness. It is found that the ensemble negative trion lifetimes reach a maximum (~4.5 ns) for an intermediate shell thickness. This leads to the smallest particles (~4.5 nm) with the brightest trion to date. Single dot measurements show that the negative charge suppresses blinking and that the trion can be as bright as the exciton at room temperature. In contrast, the biexciton lifetimes remain short and exhibit only a monotonous increase with shell thickness, showing no correlation with the negative trion decays. The suppression of the Auger process in small negatively charged CdTe/CdSe quantum dots is unprecedented and a significant departure from prior results with ultrathick CdSe/CdS core/shell or dot-in-rod structures. The proposed reason for the optimum shell thickness is that the electron–hole overlap is restricted to the CdTe core while the electron is tuned to have zero kinetic energy in the core for that optimum shell thickness. The different trend of the biexciton lifetime is not explained but tentatively attributed to shorter-lived positive trions at smaller sizes. These results improve our understanding of multiexciton recombination in colloidal quantum dots and may lead to the design of bright charged QDs for more efficient light-emitting devices.

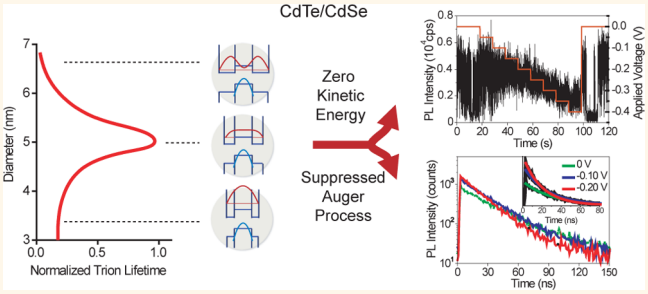

KEYWORDS: electrochemistry · Auger process · negative trion · biexciton · single dot · nonblinking

The Auger process is a three-particle process in which the recombination energy of an electron–hole pair is transferred to a third carrier (hole or electron) instead of a photon.[1] In bulk semiconductors, due to momentum conservation, the Auger process requires an activation energy which is proportional to the band gap, and therefore, in wide band gap semiconductors, it is not efficient enough to compete with the radiative recombination.[2,3] Nonetheless, colloidal quantum dots[4−6] show weak multiexciton emission[7] and low brightness of trions,[8] both of which are typically unfavorable to the development of QD-based low-threshold lasers,[7,9,10] light-emitting diodes,[11−13] and efficient photovoltaics.[14−16] These effects are typically attributed to the fast Auger process which is generally characterized by the biexciton lifetimes, following a rather universal cubic power-law increase with particle size for both direct and indirect band gap semiconductors.[5] This is qualitatively rationalized by the effective high carrier density, the confinement-induced mixing of different momentum states, and the enhanced Coulomb interaction in small semiconductor nanocrystals.[2,5,17] Inconsistencies in the description of biexciton decay in terms of the Auger process have also been noted,[6] and in some cases, the surface states have been proposed to assist the Auger recombination.[18−20] Nevertheless, strongly reduced biexciton recombination rates have been achieved but only for the very thick shell CdSe/CdS nanocrystals[21,22] and dot-in-rod structure[23] and with the loss of electron confinement. Alternatively, QDs with alloyed structures have been proposed to reduce the Auger rates by softening the confining potential sharpness and reducing the overlap between the low-energy states of the exciton and the high-energy carrier states after the Auger process.[24] However, it is still an experimental challenge to correlate the extent of alloying with the changes in the Auger recombination.[25−27]

With two electrons and one hole, the negative trion is arguably the simplest system to study the Auger process in colloidal QDs. Previously, only the type-I CdSe/ZnS and quasi-type-II CdSe/CdS have been charged

* Address correspondence to pgs@uchicago.edu.

Received for review July 26, 2013 and accepted December 14, 2013.

Published online December 14, 2013
10.1021/nn403893b

negatively by electrochemistry[27−31] or photocharging.[32−34] In the CdSe/CdS system, the trion lifetime lengthens as the CdS shell becomes thicker,[29−31] in accord with the biexciton lifetime even though the trion lifetimes are significantly longer.[8,29,30] Particularly, with very thick shell CdSe/CdS, negative trions of 100% quantum efficiency have been reported at cryogenic temperature.[31−33] With CdSe/CdS, nonradiative multicarrier recombination has been proposed to be caused by an enhanced Auger process at the abrupt outer shell surface.[32] This mechanism implies the need to prevent the electron from sampling the outer surface, calling for thick shell. However, this results in no or weak confinement, and it also suggests the impossibility of designing small charged bright dots.

The strongly type-II CdTe/CdSe QD is an interesting alternative system to study the Auger process because it takes only very small shell thicknesses to shift the electron from the CdTe core to the CdSe shell and to tune the electron energy over a very wide range, from above to below the CdTe conduction band, while the hole remains localized in the core.[35−38] Therefore, following literature protocols,[36,37] we synthesized CdTe/CdSe QDs with various shell thickness for two specific core size (3 and 4 nm). Electrochemistry has been used extensively to inject electrons into colloidal quantum dots with tunable charging levels,[39,40] and in combination with confocal fluorescence microscopy, it has recently been possible to measure the carrier dynamics in both single- and ensemble-charged QDs.[27−31] In this work, we use this spectro-electrochemical technique[27−31] to study the negative trion lifetime of the CdTe/CdSe, and ensemble results are complemented with single dot studies.

RESULTS AND DISCUSSION

Optical Absorption and Photoluminescence of Solutions and Bleach Spectra of Charged Films. As the CdSe shell thickness is increased to 4.5 monolayers with a 3 nm CdTe core, the reduced overlap between the electron and hole envelope wave functions leads to strongly redshifted absorption spectra by up to 0.7 eV (Figure 1a, top panel), while the photoluminescence (PL) lifetime slows down from ~30 to ~90 ns (Figure 1b and Supporting Information S1). This is due to the strong type-II band alignment and is consistent with previous investigations on the CdTe/CdSe QDs.[35,36]

To confirm the possibility of electron injection in these colloidal QDs, we combined electrochemistry and optical absorption spectroscopy.[8,39] Since the electron transport in the multilayer film of CdTe/CdSe QDs (3 nm/2.5 ML) under electrochemistry is relatively slow, the absorption spectra are measured at different times at a fixed potential. As seen in Figure 1a (bottom panel), taken at the potential at −1.2 V with respect to a silver wire pseudoreference electrode, the bleach

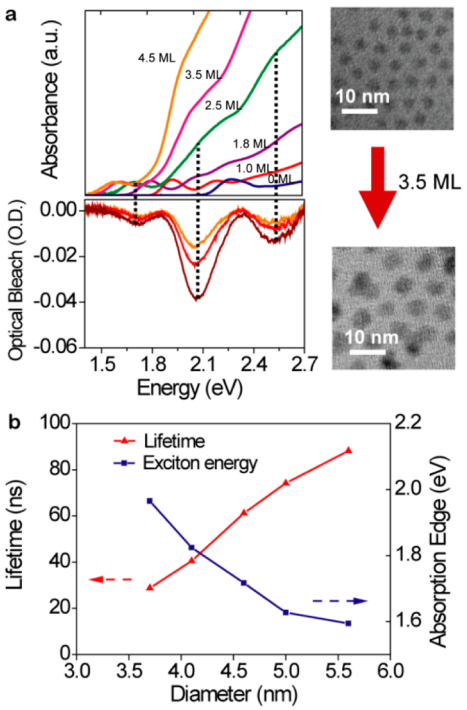

Figure 1. (a) Top graph shows the absorption spectra for CdTe/CdSe QDs in solution, with the same 3 nm core but different shell thickness (from 0 to 4.5 ML). The bottom graph shows the absorption bleach spectra of the CdTe/CdSe QDs (3 nm/2.5 ML) in a film at different times with 30 s intervals at −1.2 V. The corresponding TEM images for CdTe/CdSe QDs are also shown (top, 3 nm/1 ML; bottom, 3 nm/4.5 ML). (b) Size dependence of PL lifetime and band-edge absorption energy, measured for CdTe/CdSe QDs with 3 nm core in solution.

spectra show three peaks that evolve simultaneously as the QDs get charged. These peaks are therefore assigned to transitions between the lowest energy electron state, being occupied under the reducing potential, and three distinct hole states in the CdTe core,[37] which also confirms the expected strong hole confinement.

Ensemble PL Changes under Electrochemistry. Having verified the possibility of electron injection in films by direct absorption measurements, the photoluminescence intensity and lifetime were then measured as a function of the applied reducing potential for submonolayer samples with two different core sizes and systematically varying shell thickness. The systems were first characterized with ensemble PL measurement. In this case, a submonolayer QD film is drop-casted on an ITO substrate which has first been drop-casted with a thin layer of ZnO nanocrystals.[27−29] The ZnO layer serves to mitigate the energy transfer from QDs to the ITO while retaining electron transfer with the substrate. The QD submonolayer allows for greater PL signal than single dots while minimizing energy transfer between dots.

Figure 2a shows the typical PL intensity of CdTe/CdSe QDs as a function of potential after several

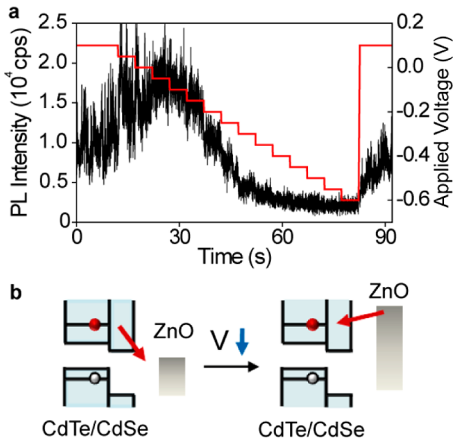

Figure 2. (a) Typical PL trace of CdTe/CdSe QDs (3 nm/4.5 ML) submonolayer films under electrochemical control. The red solid lines represent stepwise changes in applied voltage from 0.1 to −0.6 V (50 mV for each step). (b) Relative changes in energy levels for CdTe/CdSe QDs (blue) and ZnO film (gray) are shown in the schematic sketch, as the electrochemical voltage decreases. The red arrows illustrate the directions for electron transfer.

electrochemical cycles in the oxygen-free electrolyte. As the potential is made more reducing (negative), the PL initially increases slightly and then decreases significantly. Prior cycling is necessary as samples prepared on the electrodes in air are otherwise weakly luminescent, in contrast to samples on plain glass coverslips which remain bright. All CdTe/CdSe samples in this study displayed the initial rise of the PL with increasingly negative potential on the electrode. This is in contrast to CdSe/ZnS QDs which show a steady PL intensity before electron injection (Supporting Information Figure S5). A possible scenario is that electron transfer from the photoexcited dot to the ZnO substrate occurs readily for CdTe/CdSe due to the favorable band alignment (Figure 2b and Figure S6).[41,42] This would also explain the weak PL in air on the conductive electrodes as surface oxidation by the hole in the CdTe/CdSe QDs would follow the electron transfer.[29] In oxygen-free conditions, as the ZnO Fermi level is raised further, upon more negative potentials, the electron transfer is simply less efficient and the PL therefore increases. At more reducing potential, as electrons are injected into the QDs, the PL intensity drops and the lifetime shortens due to the formation of negative trions (Figure 2b).

Slow Negative Trion Decays at a Specific Shell Thickness. Figure 3a shows the very different PL decay traces of CdTe/CdSe samples with the same core size of 3 nm but different shell thickness (2.5 ML CdSe shell, left panel; 4.5 ML, right panel). The decay traces contain a slow component, which is the neutral dot PL decay in this environment, and a faster component, which is assigned to the PL decay of charged dots, as its strength increases with more negative potential. Over a range of potential, the lifetime for the faster component is then extracted as an estimation of the singly charged trion lifetime. When charging single QDs by electrochemistry, the electron injection voltage may vary significantly from dot to dot, which may be related to the local environment.[28,30] Therefore, the ensemble measurement includes a distribution of dots in different charged states. The lifetime is then a lower limit for the negative trion lifetime since it also contains the contribution from multiply charged dots, although these may be weaker emitters (see Supporting Information). The significant observation is that the PL decay of charged states is much slower for the sample with the thinner shell (Figure 3a,b). As shown in Figure 3c, comparing the results for the several shell thicknesses, it is apparent that the trion lifetime peaks at an intermediate thickness. Furthermore, this is consistent for two sets of samples with 3 and 4 nm core diameters, synthesized from two different methods.[36,37] Compared to the typical value of CdSe/CdS[8,29,30] and CdSe/ZnS[27] QDs with thin shells for which the negative trion lifetime is shorter than 1 ns, the maximum ensemble trion lifetime of ~4.5 ns is much longer and this is achieved with a very small particle size CdTe/CdSe (~4.5 nm). To our knowledge, this is the first instance of colloidal QDs with such small sizes, in which the Auger recombination rate is largely reduced.

We note that the lattice mismatch between the CdTe and CdSe could possibly lead to a critical thickness of the shell before defects or a different growth mode appears[36] and that this might cause the peaked trion lifetime. However, TEM observation confirms the spherical growth (Supporting Information Figures S2 and S4), while the PL quantum yields of all CdTe/CdSe samples in solution remain similar as the shell grows (see Supporting Information Figure S1b). Therefore, we do not assign the peak of the trion lifetime to a structural effect. With regards to the theoretical possibility of slowing down the Auger recombination with interfacial alloying,[24] the fact that the CdTe/CdSe QDs with two core sizes were obtained from different synthetic methods make it very unlikely that the degree of alloying at the interface, if any, is similar in both sets of samples and that it might peak at some thickness. Therefore, we also do not assign the long trion lifetimes to alloying effects. Finally, the observation of an optimum shell thickness departs from previous notions that the reduced overlap of the electron−hole envelope function is sufficient to slow down the nonradiative Auger process[21,23,35,43] or that the remoteness of the outer surface is essential.[32]

In the CdTe/CdSe trion, the hole state is strongly confined in the CdTe core, and it should be well-described by the heavy hole approximation being mostly a p-Bloch function. Therefore, the electron−hole overlap, important for PL as well as for the Auger recombination, is primarily in the core. The monotonous increase of the PL lifetime with shell thickness

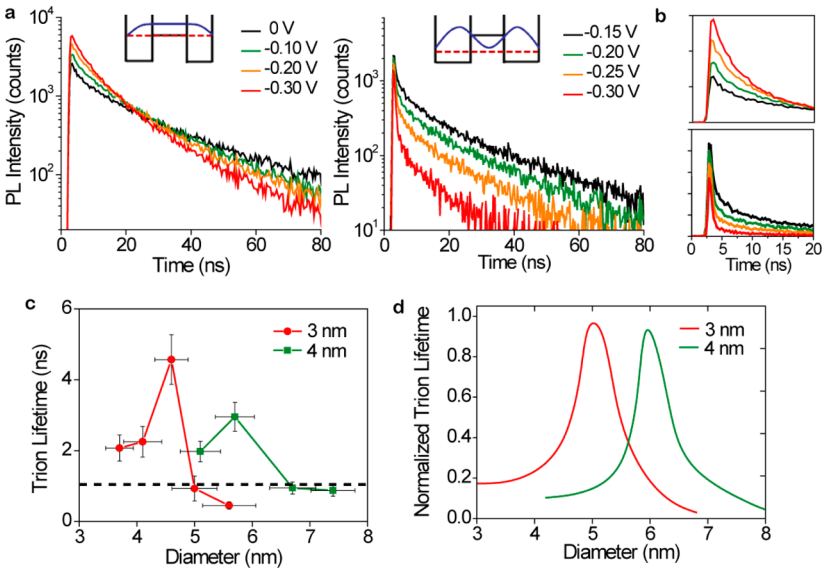

Figure 3. (a) PL lifetime traces of CdTe/CdSe at different electrochemical potentials on a semilogarithm scale (left, 4 nm/2.5 ML; right, 4 nm/4.5 ML, corresponding to the PL traces in Figure S6b,c). The sketches illustrate the corresponding band gap alignment for these samples, with the red dashed lines as the electron energy positions and the blue lines as the electron envelope wave functions. (b) Same lifetime traces as in (a) on the linear scale. (c) Ensemble trion lifetimes for all samples studied. The dashed line indicates the typical upper limit (1 ns) for trion lifetimes reported previously for particles of similar sizes. (d) Theoretical calculation for trion lifetime, with a two-band $k \cdot p$ model.

reflects the decreased envelope function overlap and dipole matrix element as the electron leaks out more into the shell.[35] However, we suggest that the nonmonotonous trion lifetime reflects the fact that it is the Bloch function overlap that is of importance for the Auger matrix element. At a specific shell thickness, the kinetic energy of the electron is zero in the core and the electron matches the bottom of the CdTe conduction band. In this case, the electron Bloch function has exactly zero p-component in the core and therefore zero overlap with the heavy hole wave function even though their envelope functions have significant overlap. On the other hand, at zero shell thickness where the electron state is strongly confined in the CdTe core, and at a thick CdSe shell where the electron energy drops below the CdTe conduction band minimum, the electron Bloch function has nonzero p-component in the core, leading to a significant overlap with the hole state (Supporting Information Figure S11). The results of calculations using a two-band $k \cdot p$ model[2,17,24,44] are shown in Figure 3d (right panel) and qualitatively agree with the experimental observations for both core sizes.

From another perspective, since the electrons are at the bottom of the conduction band at an optimum shell thickness, the Auger decay in the CdTe/CdSe QDs becomes analogous to the case for bulk semiconductor, which demands an activation energy proportional to the band gap.[2,3] The effect may also contribute to the reduced Auger rate observed in alloyed nanocrystals since the confinement typically goes down in those systems[26,27] and to the suppressed Auger process in the bulk-like CdSe/CdSe thick shell structure[21,22] and dot-in-rod structure,[23] where the electron energy is very close to the bottom of the conduction band in the CdSe core. In this regard, the nonmonotonous trend in trion lifetimes of CdTe/CdSe QDs may be the first instance where a connection in the Auger recombination between bulk semiconductors and small colloidal QDs can be firmly established.

Fast Biexciton Decays. Having achieved some success with the control of the negative trion lifetime, it seems that the biexciton lifetime should also be understood. The PL biexciton lifetimes for CdTe/CdSe QDs were then measured for samples in solutions and extracted from the fast component which appears under higher laser excitation power (Supporting Information Figure S8).[4] As shown in Figure 4, the biexciton lifetimes are much shorter than the negative trion lifetimes except for the larger sizes where they are similar. Within the measurement error, there is no difference between the two cores other than the overall size. They also show a monotonous increase with particle sizes, which is in agreement with previous experimental results on this type-II system[35] and the universal cubic size dependence of Auger rate in colloidal QDs,[5] but it does not correlate with the peaked trend of the negative trion lifetimes.

One mechanism for the biexciton decays involves surface states which can assist the fast nonradiative Auger recombination.[18−20] Even though the influence of surface chemistry and hole traps on the biexciton rate is often not observed,[6,45] trap-assisted Auger recombination has been proposed recently for ZnO colloidal nanocrystals.[19] In our study, the trion decay originates from negatively charged CdTe/CdSe dots

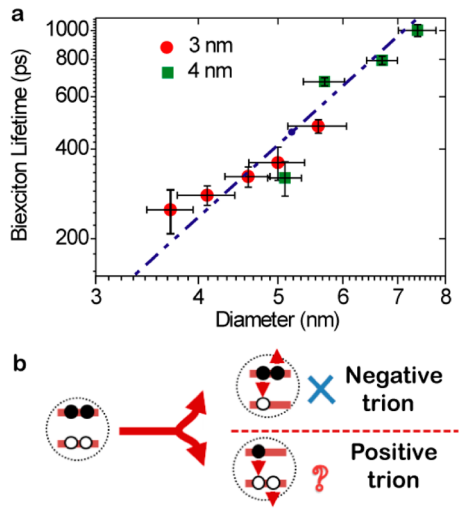

Figure 4. (a) PL biexciton lifetimes as a function of the CdTe/CdSe particle diameters. The dashed line is $\tau_{biexciton} = AD^n$, where D is the particle diameter, $n = 2.5$, and A is a constant. (b) Two possible pathways of biexciton decay in colloidal QDs.

and its Fermi level is well-defined by electrochemistry, in which case the involvement of surface traps should be greatly eliminated.[29] A possible concern is that biexciton lifetimes were measured in solution under high laser power without the knowledge of the Fermi level. Considering these facts, the PL biexciton lifetimes were also measured for submonolayer film samples under the electrochemical control. The biexciton decay was observed at higher excitation power as long as the potential was not sufficiently negative to inject electrons, and no significant differences were observed from the value of QDs in solution without potential control (Supporting Information Figure S9). Therefore, the trap-assisted Auger process also does not readily explain the monotonous trend of the biexciton lifetimes and its lack of correlation with negative trion lifetimes for this system.

Biexciton decay is more generally ascribed to two parallel channels: positive trion and negative trion decays (Figure 4b). Fast biexciton decay and slow negative trion decays have been reported before for CdSe/CdS[8,29,31] with the conclusion that the positive trion should have the faster decay.[31] Possibly, the biexciton Auger decay in the smaller CdTe/CdSe is dominated by a much faster positive trion decay. Applying the simple two-band $k \cdot p$ model as above to the positive trion leads however to the same optimum shell thickness since the recombining electron–hole overlap remains the same in the Fermi's Golden Rule integral. The model is therefore unable to describe the biexciton decay. Previous studies have already shown a puzzling insensitivity of the biexciton rate to even the gross features of the hole wave function.[6] We note that the heavy hole mass leads to small confinement energies compared to their Coulomb interaction. This suggests that hole–hole correlations may be important in the positive trion decay in nanocrystals, and this is not included at all in the single electron description of the wave functions in the Auger matrix element. Overall, the fast biexciton decay, its monotonous increase with shell thickness or size, and the lack of correlation with the peaked trend observed for the negative trions remain an unexplained result of this work.

Single Dot with Bright Nonblinking Negative Trion. At the single dot level, CdTe/CdSe QDs with the optimum shell thickness should show the same long trion lifetime. However, single dot measurements on the CdTe/CdSe systems are challenging due to the high-power excitation and photostability requirements. Although it has been reported that single CdTe/CdSe dots can withstand high illumination at cryogenic temperature,[38] the photostability of our samples is poor at room temperature. By growing a thin ZnS layer over the CdTe/CdSe QDs (Supporting Information Figure S1),[46] it was found that the photostability of the CdTe/CdSe QDs could be increased sufficiently so that single dot PL measurements could be achieved. Even though the PL of many single CdTe/CdSe/ZnS dots is still quenched on ZnO, some dots are photostable enough to be measured under electrochemical control. The PL trajectory shown in Figure 5a is for a particular single CdTe/CdSe/ZnS dot.

It shows the usual blinking between "on" and "off" state, but when the voltage is below −0.10 V, the blinking stops completely. As the voltage is brought back, the blinking recovers instantly, indicating the reversible charging process. In Figure 5b, the PL spectrum is centered at 716 nm, indicating that the dot is indeed CdTe/CdSe/ZnS and not the CdSe/ZnS dot which may exist due to homogeneous nucleation during the synthesis.

The lifetime trace at −0.20 V shows both the increased maximum photon counts by about a factor of 2 and a shorter lifetime, compared to that at 0 V at room temperature (Figure 5c), confirming the formation of singly charged negative trion at −0.20 V.[29−31,47] The trion lifetime is fitted to 20 ns at −0.20 V, while the PL lifetime from the neutral dot at 0 V is 30 ns. After accounting for the energy transfer to the ITO/ZnO substrate, the trion lifetime is calculated to be 30 ns, which is about half of the PL lifetime for single dots on bare glass (~60 ns; see Supporting Information Figure S10). This indicates that the Auger recombination is extensively suppressed in this negatively charged single dot. It is also consistent with the observation that the singly charged dot at −0.20 V is almost as bright as the "on" state at 0 V in the PL trajectory, which would imply a nearly 100% quantum yield of the negative trion at room temperature if the neutral on state is that bright. The radiative lifetime is determined by the recombination between the two

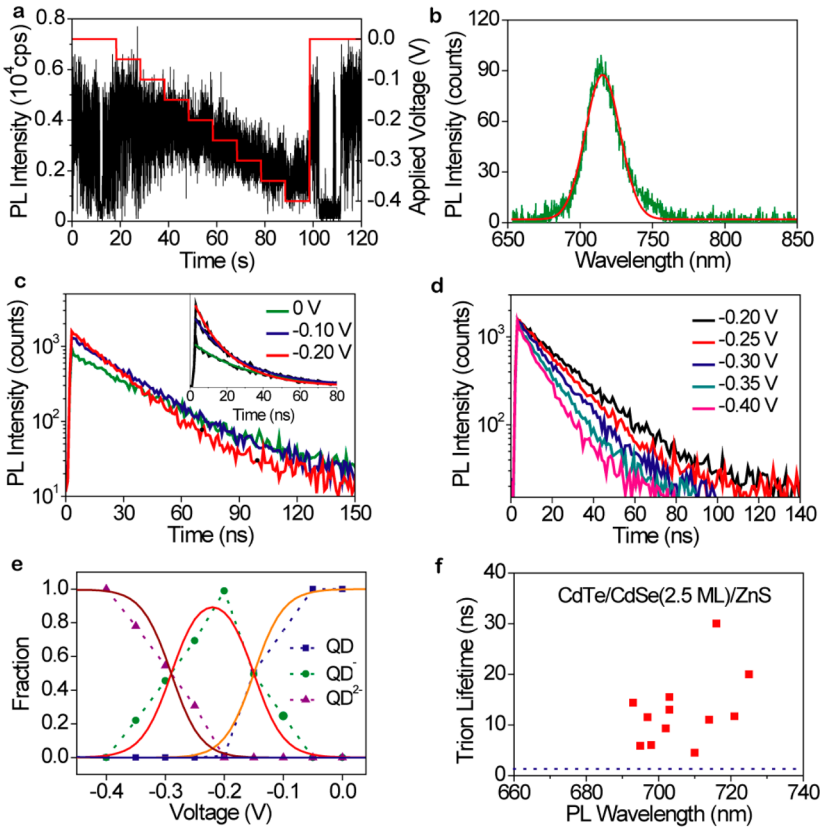

Figure 5. Single dot PL from CdTe/CdSe (3 nm/2.5 ML) overcoated with a thin ZnS shell. (a) PL trajectory of a single dot under electrochemical control. The red line shows the stepwise voltage changes from 0 to −0.4 V (50 mV per step). (b) PL spectrum for the neutral single dot with a Gaussian fit (red line, fwhm = 28 nm). (c) Lifetime traces from 0 to −0.20 V on a semilogarithm scale (inset: same traces on a linear scale with the corresponding fits). (d) Lifetime traces from −0.20 to −0.40 V. (e) Fractions of neutral, singly charged, and doubly charged states for the single dot as a function of applied voltage. The solid lines are the corresponding fits using the Nernst equation with the initial electron injection voltage of −0.15 V and a charging energy of 140 meV. (f) Trion lifetimes of different single dots as a function of their PL wavelength. The blue dashed line is the typical upper limit (1 ns) for the trion lifetime of single dots from CdSe/ZnS or CdSe/CdS (thin shell) dots.

electrons in the lowest electronic state ($1S_e$) and one hole in the highest hole state ($1S_h$), which should be the same for different charged states.[29] In Figure 5d, this can be directly verified by the constant maximum photon counts in the lifetime traces from −0.20 to −0.40 V, where up to two electrons are injected into the single dot, even though the nonradiative rate increases.

All the lifetime traces from 0 to −0.40 V can be fitted with three lifetime constants: 30, 20, and 10 ns, assigned to the neutral, singly charged, and doubly charged states (Supporting Information Table 1). The coefficients, obtained from fitting the lifetime traces, can be then used to calculate the relative fractions of the charged states,[29] whose evolution with voltages is well-described by the Nernst equation, identifying a charging energy of 140 meV. Compared to the typical value for large-size QDs (30−80 meV),[8,29] this charging energy reflects the small particle size of this single dot (~4 nm).

All the single dots within the same batch of the optimum thickness (3 nm/2.5 ML) that could be measured showed suppressed blinking in the trion state (Supporting Information Figure S11). While the very long trion lifetime discussed above was unique among the single dots studied, the distribution of trion lifetimes does show a large variation from 5 to 30 ns with relatively small changes in the corresponding PL wavelength (Figure 5f), possibly due to the small variations in core sizes and shell thickness. The range of the PL wavelength for those single dots (~0.06 eV) is smaller than the PL shift due to a monolayer increase of the CdSe shell (~0.11 eV). The wide range of trion lifetimes is consistent with the expectation that electron energy is in the vicinity of the bottom of the bulk CdTe conduction band for these CdTe/CdSe (3 nm/2.5 ML) dots, and that the Auger decay is very sensitive to the relative positions of electron energy. In contrast, single dots of the batches with smaller or larger shell thicknesses showed consistently short trion lifetimes of 1 ns or less.

CONCLUSIONS

In summary, we observed a maximum of the lifetime of negative charged CdTe/CdSe dots with a specific shell thickness. This was verified by making two series of core/shells with a different core size and different

synthetic protocols. At the single dot level for CdTe/CdSe/ZnS, this leads to the interesting observation of small, bright, nonblinking charged single dots with similar brightness as the neutral dots at room temperature. Using the simplest $k \cdot p$ model, the suppression of the negative trion Auger process is proposed to arise from the zero kinetic energy of the electron state in the core, which is possible in strong CdTe/CdSe or weak CdSe/CdS type-II core/shell structure for a specific shell thickness while the hole is strongly confined to the core.

However, the biexciton lifetimes on the same systems exhibit a monotonous trend with shell thickness, and this is not explained. In the cadmium chalcogenide system, the positive trion is not accessible; therefore, the discrepancy cannot be investigated further. Future experiments may be able to compare the trion and biexciton rates in other systems and to compare positive and negative trions. Alternatively, it may well be that the larger density of hole states leads to qualitative differences between positive trions and negative trions or biexcitons due to correlation and polaronic effects.

While previous studies achieved nonblinking bright trion states in some ultrathick shell weakly type-II CdSe/CdS systems and at cryogenic temperature, the strongly type-II CdTe/CdSe affords smaller dots with a nonblinking negative trion as bright as the exciton at room temperature. With improvement in photostability, the new design for Auger suppression might help the development of colloidal QD-based LEDs[11] and single photon sources.[48]

METHODS

Synthesis of Colloidal QDs. All chemicals were purchased from Sigma-Aldrich without further purification. Cadmium stock solution (0.1 M) was prepared by dissolving CdO (1 mmol, 128.4 mg) in OA (4 mmol, 1.3 mL) and ODE (9 mL) at 240 °C under argon atmosphere and stored in the air. Selenium stock solution (0.085 M) was prepared by dissolving selenium (0.9 mmol, 71.0 mg) in 1.6 mL of TOP and 9 mL of ODE with stirring in the glovebox. ZnS precursor stock solution (0.1 M) was prepared by dissolving zinc diethyl dithiocarbamate in TOP and ODE (v/v, 1:1) at 100 °C in the glovebox. All the preparations of tellurium solution were manipulated in the glovebox. The CdTe/CdSe nanocrystals with different core sizes were synthesized according the previous methods,[36,37] with minor modifications.

Synthesis of CdTe/CdSe Nanocrystals with 3 nm Core[36]. Cadmium stock solution (0.1 M, 2 mL) and 1 mL of ODE were degassed under vacuum at 100 °C for 20 min. Refilled with argon, the solution was heated to 280 °C after which the solution with tellurium (0.1 mmol, 12.8 mg) and ODPA (0.15 mmol, 50.2 mg) dissolved in 0.15 mL of TOP and 1 mL of ODE was added quickly. The reaction was maintained at 280 °C for 3 min and cooled rapidly to room temperature to quench the particle growth. This would produce a CdTe core with the absorption edge at 535 nm, corresponding to the average size of 3 nm. In order to synthesize CdTe/CdSe with different shell thickness, half of the raw CdTe core solution was degassed at 100 °C for 20 min and then heated to 230 °C under argon atmosphere. Equivalent amounts of cadmium and selenium stock solution were added alternatively to the reaction solution with the injection speed of 3 drops per 1 min for each precursor. The CdTe/CdSe samples of different shell thickness investigated corresponded to the addition of 1, 2, 3, 5, and 7 mL for each precursor in the shell growth solution.

Synthesis of CdTe/CdSe Nanocrystals with 4 nm Core with SILAR Technique[37]. Under vacuum, the mixture containing cadmium oxide (0.1 mmol, 12.8 mg), TDPA (0.22 mmol, 61 mg), and 5 mL of ODE was heated to 100 °C for 20 min. The solution temperature was then increased to 300 °C under argon. After a clear solution was obtained, the temperature was decreased to 280 °C and a solution of tellurium (0.2 mmol, 25 mg) dissolved in 0.6 mL of TBP and 1.9 mL of ODE was injected swiftly. The temperature dropped to 250 °C and was maintained for 20 min to produce CdTe nanocrystals with the absorption edge at 630 nm and the average size of 4 nm. The reaction solution was then cooled to room temperature to quench the particle growth. After precipitation from the solution by adding ethanol and centrifugation, the CdTe nanocrystals were redissolved in tetrachloroethylene, precipitated by adding acetone and centrifuged again. Finally, the CdTe nanocrystals were dissolved in chloroform. The amount of CdTe nanocrystals in the chloroform solution was determined by measuring the absorbance at the band-edge wavelength peak.

Initially, the similar strategy to add each precursor dropwise and consecutively was used to grow a CdSe shell on the 4 nm CdTe core. However, the reaction always resulted in the appearance of PL at about 550 nm and almost no shifts of the PL wavelength from CdTe nanocrystals in the PL spectrum, indicating the homogeneous nucleation of CdSe precursors instead of heterogeneous nucleation on CdTe nanocrystals. A possible reason is that the reaction of Cd and Se precursors on CdTe nanocrystals is very slow when compared to homogeneous nucleation. Therefore, the SILAR technique was applied for the 4 nm CdTe core to grow the CdSe shell. Typically, the chloroform solution of CdTe nanocrystals was added to the flask containing 3 mL of ODE and 1.5 g of ODA. The solution was degassed under vacuum to remove chloroform and heated to 100 °C for 20 min. The solution was then heated under argon to 240 °C, in which the cadmium stock solution for the growth of one monolayer of CdSe shell was added. The solution was maintained for 40 min, and then the selenium stock solution was added. After the addition of each precursor, the reaction was maintained for 40 min. The procedure was repeated to achieve the desired shell thickness. For each CdSe shell growth, the amounts of cadmium and selenium stock solution added to the solution were calculated according to the concentration of CdTe core and its particle size. In addition, 10% excess of the calculated amount of cadmium stock solution was actually injected in order to make selenium consumed completely.

Synthesis of CdTe/CdSe/ZnS Nanocrystals with 3 nm Core[46]. In order to increase the photostability of CdTe/CdSe nanocrystals, the growth of the thin ZnS shell on plain CdTe and CdTe/CdSe (2 ML) nanocrystals was accomplished by using previous methods with small changes. In general, the core nanocrystals, after cleaning by precipitation, were dissolved in 3 mL of ODE with ODPA (0.075 mmol, 25 mg) and oleic acid (0.13 mL, 0.4 mmol). The solution was degassed under vacuum at 100 °C for 20 min and refilled with argon. As soon as the temperature was increased to 135 °C, 0.15 mL of ZnS precursor solution was injected. After 5 min, the solution was heated to 200 °C for another 5 min. As the solution was maintained at 200 °C, another 1.85 mL of ZnS precursor solution was added to the solution dropwise and slowly in 1 h to eliminate the possibility of homogeneous nucleation of ZnS. Due to the relative large lattice mismatch (~16%) between CdTe and ZnS, only a thin ZnS shell (<1 ML) growth can be achieved.

Electrochemical Cell Setup. The electrochemical experiments were performed in an airtight electrochemical cell with the platinum wire as counter electrode, a cadmium wire as pseudo-reference electrode, and ITO coverslips as working electrode.

The electrolyte used is tetrabutylammonium perchlorate (dried 12 h at 0.1 Torr and 100 °C) dissolved in anhydrous propylene carbonate (0.1 M). The ZnO cross-linked film (~20 nm thickness, ~7 nm roughness) was prepared on ITO coverslips following the methods described previously.[27−29] The films for PL measurements of ensembles and single dots were drop-casted on ITO/ZnO substrates by controlling the concentration of QDs in hexane/octane (9:1) and cross-linked by treating with 1,7-diaminoheptane in ethanol (1%, v/v). Typically, there are ~10 single dots within the confocal spot in the ensemble measurements, and the trion lifetimes given in the figures are averaged by measuring different regions of the same sample.

Optical Microscopy. For lifetime measurements under electrochemistry, the quantum dot films were excited by a 405 nm pulsed diode laser (Hamamatsu, 45 ps pulse duration, 5 MHz repetition rate). The excitation power was ~0.5 kW/cm^2. With a confocal fluorescence microscope, the PL was collected by an infinity-corrected oil immersion objective (Olympus, NA 1.40, 60×) and separated by a 50:50 beam splitter for simultaneous collection on an APD (PerkinElmer) and CCD camera (Andor). To obtain PL trajectories and lifetime traces simultaneously, time-tagged/time-resolved (TTTR) mode with PicoQuant PH 300 was used, in which photon delay times with regard to both the starting point of the measurement and each laser pulse were recorded. The raw TTTR data were analyzed with software written in C++.

PL Biexciton Lifetime Measurement. In order to measure the biexciton lifetimes in QD solution, a piece of glass coverslip was glued to a microscope glass slide on the edges, thus creating a small gap liquid cell. The gap was filled with a CdTe/CdSe QD solution in tetrachloroethylene. The Ti:sapphire laser (Coherent Mira, 75.5 MHz, <200 fs pulse width) was doubled to 425 nm and focused by an infinity-corrected objective (Nikon ELWD, NA 0.80, 100×, 3.5 WD) to excite the thin layer of solution. PL decay traces were recorded by a Picoquant MPD avalanche photodiode at 16 ps time resolution. The instrument response function was measured with the fwhm of 110 ps. The excitation power was adjusted by a neutral density filter, and biexciton PL decay is generated by raising the excitation power and extracted by subtracting the normalized PL decay at lower excitation power. After high-power excitation, the samples were excited again at low power to verify the absence of photodegradation at high power. Under the excitation of a Ti:sapphire laser, biexciton lifetimes under potential control were extracted similarly from the submonolayer film as for ensemble trion lifetime measurements.

Conflict of Interest: The authors declare no competing financial interest.

Acknowledgment. W.Q. acknowledges the financial support from the Petroleum Research Fund under Grant ACS-PRF 51312-ND10. H.L. acknowledges the support from the DOE under Grant No. DE-FG02- 06ER46326.

Supporting Information Available: PL lifetime traces for solution, TEM images, PL trajectories for single dots and ensembles under electrochemistry, PL biexciton decay traces, details for calculation of Auger recombination in the negative trion decay. This material is available free of charge *via* the Internet at http://pubs.acs.org.

REFERENCES AND NOTES

1. Landsberg, P. T. *Recombination in Semiconductors*; Cambridge University Press: Cambridge, UK, 1991.
2. Klimov, V. I. *Nanocrystal Quantum Dots*, 2nd ed.; CRC Press: Boca Raton, FL, 2009.
3. Abakumov, V. N. In *Nonradiative Recombination in Semiconductors*; Perel, V. I., Yassievich, I. N., Eds.; Elsevier Science Pub: Amsterdam, 1991.
4. Klimov, V. I.; Mikhailovsky, A. A.; McBranch, D. W.; Leatherdale, C. A.; Bawendi, M. G. Quantization of Multiparticle Auger Rates in Semiconductor Quantum Dots. *Science* **2000**, *287*, 1011–1013.
5. Roble, I.; Gresback, R.; Kortshagen, U.; Schaller, R. D.; Klimov, V. I. Universal Size-Dependent Trend in Auger Recombination in Direct-Gap and Indirect-Gap Semiconductor Nanocrystals. *Phys. Rev. Lett.* **2009**, *102*, 177404.
6. Pandey, A.; Guyot-Sionnest, P. Multicarrier Recombination in Colloidal Quantum Dots. *J. Chem. Phys.* **2007**, *127*, 111104.
7. Klimov, V. I.; Mikhailovsky, A. A.; Xu, S.; Malko, A.; Hollingsworth, J. A.; Leatherdale, C. A.; Eisler, H.-J.; Bawendi, M. G. Optical Gain and Stimulated Emission in Nanocrystal Quantum Dots. *Science* **2000**, *290*, 314–317.
8. Jha, P. P.; Guyot-Sionnest, P. Trion Decay in Colloidal Quantum Dots. *ACS Nano* **2009**, *3*, 1011–1015.
9. Wang, C.; Wehrenberg, B. L.; Woo, C. Y.; Guyot-Sionnest, P. Light Emission and Amplification in Charged CdSe Quantum Dots. *J. Phys. Chem. B* **2004**, *108*, 9027–9031.
10. Liao, Y.; Xing, G.; Mishra, N.; Sum, T. C.; Chan, Y. Low Threshold, Amplified Spontaneous Emission from Core-Seeded Semiconductor Nanotetrapods Incorporated into a Sol−Gel Matrix. *Adv. Mater.* **2012**, *24*, OP159–OP164.
11. Cho, K.; Lee, E. K.; Joo, W.; Jang, E.; Kim, T.; Lee, S. J.; Kwon, S.; Han, J. Y.; Kim, B.; Choi, B. L.; *et al.* High-Performance Crosslinked Colloidal Quantum-Dot Light-Emitting Diodes. *Nat. Photonics* **2009**, *3*, 341–345.
12. Pal, B. N.; Ghosh, Y.; Brovelli, S.; Laocharoensuk, R.; Klimov, V. I.; Hollingsworth, J. A.; Htoon, H. 'Giant' CdSe/CdS Core/Shell Nanocrystal Quantum Dots as Efficient Electroluminescent Materials: Strong Influence of Shell Thickness on Light-Emitting Diode Performance. *Nano Lett.* **2012**, *12*, 331–336.
13. Iveland, J.; Martinelli, L.; Peretti, J.; Speck, S. J.; Weisbuch, C. Direct Measurement of Auger Electrons Emitted from a Semiconductor Light-Emitting Diode under Electrical Injection: Identification of the Dominant Mechanism for Efficiency Droop. *Phys. Rev. Lett.* **2013**, *110*, 177406.
14. Nozik, A. J. Quantum Dot Solar Cells. *Physica E* **2002**, *14*, 115–120.
15. Zhu, H.; Yang, Y.; Lian, T. Multiexciton Annihilation and Dissociation in Quantum Confined Semiconductor Nanocrystals. *Acc. Chem. Res.* **2013**, *46*, 1270–1279.
16. Beard, M. C.; Luther, J. M.; Semonin, O. E.; Nozik, A. J. Third Generation Photovoltaics Based on Multiple Exciton Generation in Quantum Confined Semiconductors. *Acc. Chem. Res.* **2013**, *46*, 1252–1260.
17. Chepic, D. I.; Efros, A. L.; Ekimov, A. I.; Ivanov, M. G.; Kharchenko, V. A.; Kudriavtsev, I. A.; Yazeva, T. V. Auger Ionization of Semiconductor Quantum Drops in a Glass Matrix. *J. Lumin.* **1990**, *47*, 113–127.
18. Zhao, J.; Chen, O.; Strasfeld, D. B.; Bawendi, M. G. Biexciton Quantum Yield Heterogeneities in Single CdSe(CdS) Core-(Shell) Nanocrystals and Its Correlation to Exciton Blinking. *Nano Lett.* **2012**, *12*, 4477–4483.
19. Cohn, A. W.; Schimpf, A. M.; Gunthardt, C. E.; Gamelin, D. R. Size-Dependent Trap-Assisted Auger Recombination in Semiconductor Nanocrystals. *Nano Lett.* **2013**, *13*, 1810–1815.
20. Califano, M. Off-State Quantum Yields in the Presence of Surface Trap States in CdSe Nanocrystals: The Inadequacy of the Charging Model To Explain Blinking. *J. Phys. Chem. C* **2011**, *115*, 18051–18054.
21. Garcia-Santamaria, F.; Brovelli, S.; Viswanatha, R.; Hollingsworth, J. A.; Htoon, H.; Crooker, S. A.; Klimov, V. I. Breakdown of Volume Scaling in Auger Recombination in CdSe/CdS Heteronanocrystals: The Role of the Core−Shell Interface. *Nano Lett.* **2011**, *11*, 687–693.
22. Spinicelli, P.; Buil, S.; Quelin, X.; Mahler, B.; Dubertret, B.; Hermier, J. P. Bright and Grey States in CdSe−CdS Nanocrystals Exhibiting Strongly Reduced Blinking. *Phys. Rev. Lett.* **2009**, *102*, 136801.
23. Zavelani-Rossi, M.; Lupo, M. G.; Tassone, F.; Manna, L.; Lanzani, G. CdSe/CdS Dot-in-Rods: Suppression of Biexciton Auger Recombination in CdSe/CdS Dot/Rods: Role of the Electronic Structure in the Carrier Dynamics. *Nano Lett.* **2010**, *10*, 3142–3150.
24. Cragg, G. E.; Efros, A. L. Suppression of Auger Processes in Confined Structures. *Nano Lett.* **2010**, *10*, 313–317.
25. Wang, X.; Ren, X.; Kahen, K.; Hahn, M. A.; Rajeswaran, M.; Maccagnano-Zacher, S.; Silcox, J.; Cragg, G. E.; Efros, A. L.;

Krauss, T. D. Non-blinking Semiconductor Nanocrystals. *Nature* **2009**, *459*, 686–689.
26. Bae, W. K.; Padilha, L. A.; Park, Y.; McDaniel, H.; Robel, I.; Pietryga, J. M.; Klimov, V. I. Controlled Alloying of the Core–Shell Interface in CdSe/CdS Quantum Dots for Suppression of Auger Recombination. *ACS Nano* **2013**, *7*, 311–3419.
27. Qin, W.; Shah, R. A.; Guyot-Sionnest, P. CdSeS/ZnS Alloyed Nanocrystal Lifetime and Blinking Studies under Electrochemical Control. *ACS Nano* **2012**, *6*, 912–918.
28. Jha, P. P.; Guyot-Sionnest, P. Electrochemical Switching of the Photoluminescence of Single Quantum Dots. *J. Phys. Chem. C* **2010**, *114*, 21138–21141.
29. Qin, W.; Guyot-Sionnest, P. Evidence for the Role of Holes in Blinking: Negative and Oxidized CdSe/CdS Dots. *ACS Nano* **2012**, *6*, 9125–9132.
30. Galland, C.; Ghosh, Y.; Steinbruck, A.; Sykora, M.; Hollingsworth, J. A.; Klimov, V. I.; Htoon, H. Two Types of Luminescence Blinking Revealed by Spectroelectrochemistry of Single Quantum Dots. *Nature* **2011**, *479*, 203–207.
31. Galland, C.; Ghosh, Y.; Steinbruck, A.; Sykora, M.; Hollingsworth, J. A.; Klimov, V. I.; Htoon, H. Lifetime Blinking in Nonblinking Nanocrystal Quantum Dots. *Nat. Commun.* **2012**, *3*, 908.
32. Javaux, C.; Mahler, B.; Dubertret, B.; Shabaev, A.; Rodina, A. V.; Efros, A. L.; Yakovlev, D.; Liu, F.; Bayer, M.; Camps, G.; *et al.* Thermal Activation of Non-radiative Auger Recombination in Charged Colloidal Nanocrystals. *Nat. Nanotechnol.* **2013**, *8*, 206–212.
33. Fernee, M. J.; Sinito, C.; Louyer, Y.; Potzner, C.; Nguyen, T.; Mulvaney, P.; Tamarat, P.; Lounis, B. Magneto-optical Properties of Trions in Non-blinking Charged Nanocrystals Reveal an Acoustic Phonon Bottleneck. *Nat. Commun.* **2012**, *3*, 1287.
34. Fernee, M. J.; Littleton, B. N.; Rubinsztein-Dunlop, H. Detection of Bright Trion States Using the Fine Structure Emission of Single CdSe/ZnS Colloidal Quantum Dots. *ACS Nano* **2009**, *3*, 3762–3768.
35. Oron, D.; Kazes, M.; Banin, U. Multiexcitons in Type-II Colloidal Semiconductor Quantum Dots. *Phys. Rev. B* **2007**, *75*, 035330.
36. Cai, X.; Mirafzal, H.; Nguyen, K.; Leppert, V.; Kelley, D. F. Spectroscopy of CdTe/CdSe Type-II Nanostructures: Morphology, Lattice Mismatch, and Band-Bowing Effects. *J. Phys. Chem. C* **2012**, *116*, 8118–8127.
37. Zhu, H.; Song, N.; Lian, T. Wave Function Engineering for Ultrafast Charge Separation and Slow Charge Recombination in Type II Core/Shell Quantum Dots. *J. Am. Chem. Soc.* **2011**, *133*, 8762–8771.
38. Osovsky, R.; Cheskis, D.; Kloper, V.; Sashchiuk, A.; Kroner, M.; Lifshitz, E. Continuous-Wave Pumping of Multiexciton Bands in the Photoluminescence Spectrum of a Single CdTe–CdSe Core–Shell Colloidal Quantum Dot. *Phys. Rev. Lett.* **2009**, *102*, 197401.
39. Liu, H.; Pourret, A.; Guyot-Sionnest, P. Mott and Efros–Shklovskii Variable Range Hopping in CdSe Quantum Dots Films. *ACS Nano* **2010**, *4*, 5211–5216.
40. Yu, D.; Wang, C.; Guyot-Sionnest, P. n-Type Conducting CdSe Nanocrystal Solids. *Science* **2003**, *300*, 1277–1280.
41. Robel, I.; Kuno, M.; Kamat, P. V. Size-Dependent Electron Injection from Excited CdSe Quantum Dots into TiO_2 Nanoparticles. *J. Am. Chem. Soc.* **2007**, *129*, 4136–4137.
42. Shi, A.; Sun, J.; Zeng, Q.; Shao, C.; Sun, Z.; Li, H.; Kong, X.; Zhao, J. Photoluminescence Quenching of CdTe/CdS Core–Shell Quantum Dots in Aqueous Solution by ZnO Nanocrystals. *J. Lumin.* **2011**, *131*, 1536–1540.
43. Nanda, J.; Ivanov, S. A.; Htoon, H.; Bezel, I.; Piryatinski, A.; Tretiak, S.; Klimov, V. I. Absorption Cross Sections and Auger Recombination Lifetimes in Inverted Core–Shell Nanocrystals: Implications for Lasing Performance. *J. Appl. Phys.* **2006**, *99*, 034309.
44. Efros, A. L.; Rosen, M. The Electronic Structure of Semiconductor Nanocrystals. *Annu. Rev. Mater. Sci.* **2000**, *30*, 475–521.
45. Kobayashi, Y.; Nishimura, T.; Yamaguchi, H.; Tamai, N. Effect of Surface Defects on Auger Recombination in Colloidal CdS Quantum Dots. *J. Phys. Chem. Lett.* **2011**, *2*, 1051–1055.
46. Zhang, W.; Chen, G.; Wang, J.; Ye, B.; Zhong, X. Design and Synthesis of Highly Luminescent Near-Infrared-Emitting Water-Soluble CdTe/CdSe/ZnS Core/Shell/Shell Quantum Dots. *Inorg. Chem.* **2009**, *48*, 9723–9731.
47. Rabouw, F. T; Lunnemann, P.; van Dijk-Moes, R. J. A.; Frimmer, M.; Pietra, F.; Koenderink, A. F.; Vanmaekelbergh, D. Reduced Auger Recombination in Single CdSe/CdS Nanorods by One-Dimensional Electron Delocalization. *Nano Lett.* **2013**, *13*, 4884–4892.
48. Benjamin, S. Single Photons "on Demand". *Science* **2000**, *290*, 2273–2274.